Supporting Information for "Looking for subsurface oceans within the moons of Uranus using librations and gravity"

D. J. Hemingway[1], F. Nimmo[2]

[1]Institute for Geophysics, Jackson School of Geosciences, University of Texas at Austin, 10601 Exploration Way, Austin, TX, 78758

[2]Department of Earth and Planetary Sciences, University of California Santa Cruz, 1156 High St., Santa Cruz, CA, 95064

Contents of this file

Text S1: Measurement Precision

Figure 1 in the main text illustrates how libration amplitude is expected to vary with ice shell thickness for each of the bodies we considered. If the ice shells are thin (and therefore the oceans are thick), libration amplitudes are relatively large and easily distinguished from the 'no-ocean' case. But what measurement precision is required to distinguish between the different interior models and to confirm or rule out the presence of a subsurface ocean? This depends on what part of Figure 1 we consider. Because libration amplitude

_____

August 21, 2024, 2:39pm

is an inverse function of shell thickness, the curves in Figure 1 (recognizing that this is a log-log plot) are steep when the ice shell thickness is small and flatter when the ice shells are thick (i.e., when the oceans are thin). That is, for small ice shell thicknesses, small changes in ice shell thickness result in large changes in libration amplitude. By comparison, for larger ice shell thicknesses, a much larger change in shell thickness is required to yield the same change in libration amplitude. The gradients of the curves in Figure 1 ($\frac{\partial d}{\partial \gamma}$) can thus be used to quantify the relationship between the precision of libration amplitude measurements and the resulting uncertainty in shell thickness (for a given thickness, this is very nearly equivalent to the uncertainty in ocean thickness). Considering a range of possible libration amplitude measurement uncertainties (from 1 to 100 m), we obtain the shell/ocean thickness uncertainties shown in Figure S2. Although this information is already implicit in Figure 1, Figure S2 reveals greater detail that can further clarify the relationships. Notably, if the thickness uncertainty is larger than the ocean thickness, the presence of an ocean cannot be confirmed (region above/right of the dash-dotted black line). Whereas Figure S2 assumes $\rho_{\mathrm{core}} = 2400\,\mathrm{kg\,m^{-3}}$, Figure S3 is obtained by instead assuming $\rho_{\mathrm{core}} = 3000\,\mathrm{kg\,m^{-3}}$, which may be more applicable to the larger moons depending on their thermal evolution (Castillo-Rogez et al., 2023).

The white contours in Figures S2 and S3 indicate the precision with which the ice shell thickness can be estimated under various conditions. Estimating the ice shell thickness to within 10%, for example, requires being below the dashed white line; being below the dash-dotted white line ensures estimates are within 50% of the true value. Because the gradients ($\frac{\partial d}{\partial \gamma}$) vary as a function of shell thickess, no single value of libration measurement

precision can guarantee any given desired precision in shell/ocean thickness determination.

Nevertheless, a few broad conclusions can be drawn from Figures S2 and S3. First, using

librations to confirm the presence of a subsurface ocean on Titania or Oberon may be

difficult unless the ice shells are thin or the libration measurements can be very precise

(lower left corners of those subplots). Second, results are similar across Miranda, Ariel,

and Umbriel, suggesting that one broad set of planning guidelines may be suitable for all

three. For example, if libration amplitudes can be estimated to within $\sim 10\,\text{m}$, oceans

can be detected within these bodies even for ice shell thicknesses up to $\sim 100\,\text{km}$. With

a precision of $\sim 10\,\text{m}$, libration measurements would reveal oceans as thin as $\sim 30\,\text{km}$

at Miranda or $\sim 40\,\text{km}$ at Ariel and Umbriel. This again assumes $\rho_{\text{core}} = 2400\,\text{kg}\,\text{m}^{-3}$

but if we assume $\rho_{\text{core}} = 3000\,\text{kg}\,\text{m}^{-3}$ for Ariel and Umbriel (Castillo-Rogez et al., 2023),

$\sim 10\,\text{m}$ of libration amplitude precision assures ocean detection only if oceans are at least

$\sim 60\,\text{km}$ thick. Detection of thinner oceans would require even greater precision in the

libration amplitude estimates, which could be achievable given the right instrumentation

and tour design (Park et al., 2020).

Text S2: Radiogenic Heating

Figure S5 illustrates radiogenic heat production for bodies that are a mixture of ice and

rock. We assume a mixture of water/ice with $\rho_{\text{H2O}} = 1000\,\text{kg}\,\text{m}^{-3}$ and chondritic rock

with $\rho_{\text{chond}} = 3500\,\text{kg}\,\text{m}^{-3}$ and that the radiogenic heat production rate for this rock is

$H = 4.5 \times 10^{-12}\,\text{W}\,\text{kg}^{-1}$ (Spohn and Schubert, 2003). The bodies we consider may consist

of a combination of ice, water, and porous and/or hydrated silicates, so their rocky cores

will generally not consist of purely chondritic rock. We use each body's bulk density ($\bar{\rho}$) to

compute the equivalent mass fraction of chondritic rock as $f = \frac{1/\bar{\rho} - 1/\rho_{\mathrm{H2O}}}{1/\rho_{\mathrm{chond}} - 1/\rho_{\mathrm{H2O}}}$ (Hemingway

and Mittal, 2019). The total radiogenic heat production is then simply HfM where M

is the body's total mass, regardless of the core density. This approach accounts for the

fact that a body with a lower core density (due to hydration or having ice- or water-filled

pores) produces proportionally less radiogenic heat.

Text S3: Ice Shell Rigidity

The magnitude of the radial displacements (the y values discussed in A.2.2) depend

mainly on the ice shell's rigidity and viscosity. If the ice shell has very high rigidity, y_{s}

and y_{o} will be small (y_{c} is small in any case) and the libration amplitude given by (A15)

approaches the value given by (A13). When the ice shells are thin, and especially for

the larger bodies, libration amplitudes are lower when the finite rigidity is taken into

account. For purposes of Figures 1 and 2, we adopt $\mu = 4\,\mathrm{GPa}$ and $\eta = 10^{20}\,\mathrm{Pa\,s}$ for the

ice shell but, for reference, Figures S6 and S7 illustrate the maximum possible libration

amplitudes, obtained by assuming an infinitely rigid shell and computing them instead

via (A13)—the same result is obtained with (A15) when we adopt very large μ and η.

Table S1. Satellite properties and libration amplitudes assuming no ocean. Satellite periods, eccentricities, and masses are from Jacobson (2014). Radii are from Thomas (1988), Widemann et al. (2009), and Park et al. (2024). Moments of inertia are calculated via (A2) and (A8) assuming the bodies consist of a water ice mantle ($\rho_{\mathrm{ice}}{=}930\,\mathrm{kg\,m^{-3}}$) covering a rocky core (with densities specified in the column headers). γ is calculated via (A11).

| Satellite	P (days)	e	$M(\times 10^{20}\mathrm{kg})$	R(km)	$\bar{\rho}(\mathrm{kg/m^3})$	$\rho_{\mathrm{core}}{=}2400\,\mathrm{kg\,m^{-3}}$			$\rho_{\mathrm{core}}{=}3500\,\mathrm{kg\,m^{-3}}$		
						$\frac{B-A}{C}$	$\frac{I}{MR^2}$	γR(m)	$\frac{B-A}{C}$	$\frac{I}{MR^2}$	γR(m)
Enceladus	1.3702	0.0047	1.08	252.0	1611.1	1.83e-02	0.332	137.47	1.59e-02	0.301	118.52
Miranda	1.4135	0.0014	0.64	235.8	1165.4	2.53e-02	0.343	52.26	2.47e-02	0.336	50.91
Ariel	2.5204	0.0012	12.51	578.9	1539.4	5.49e-03	0.330	23.67	4.87e-03	0.302	20.95
Umbriel	4.1442	0.0039	12.75	584.7	1522.7	2.04e-03	0.329	28.38	1.82e-03	0.303	25.26
Titania	8.7059	0.0012	34.00	788.9	1653.2	4.34e-04	0.334	2.53	3.73e-04	0.300	2.17
Oberon	13.4632	0.0014	30.76	761.4	1663.6	1.81e-04	0.335	1.16	1.55e-04	0.300	0.99
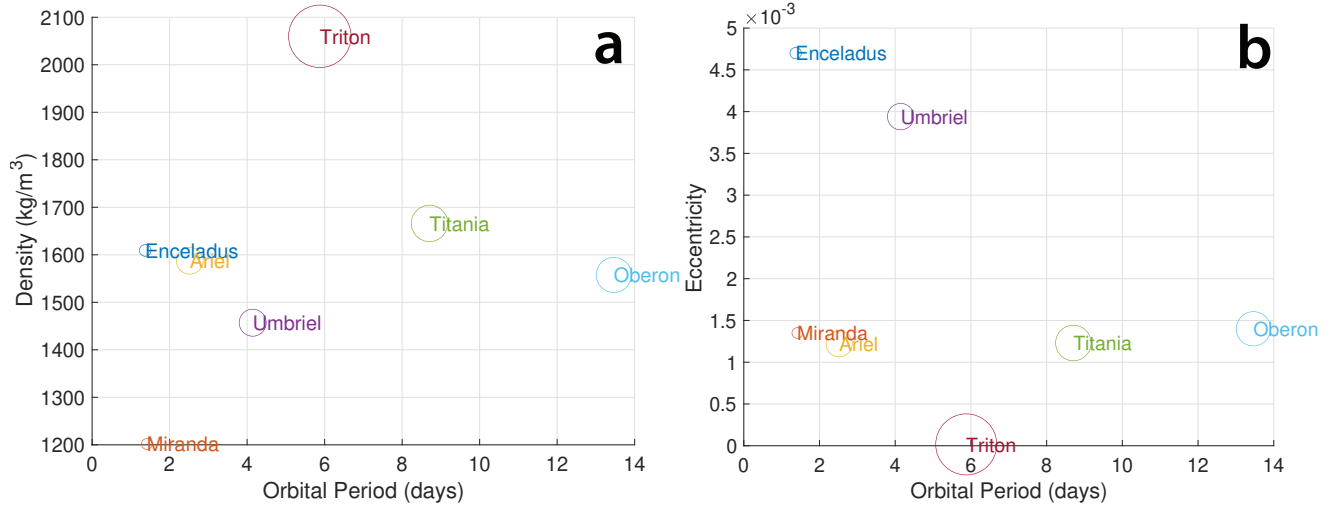
Figure S1. Orbital periods versus bulk densities (a) and orbital eccentricities (b) of the large Uranian moons plus Enceladus and Triton. Body size is indicated by the size of the circles, which are shown on an arbitrary but common scale.
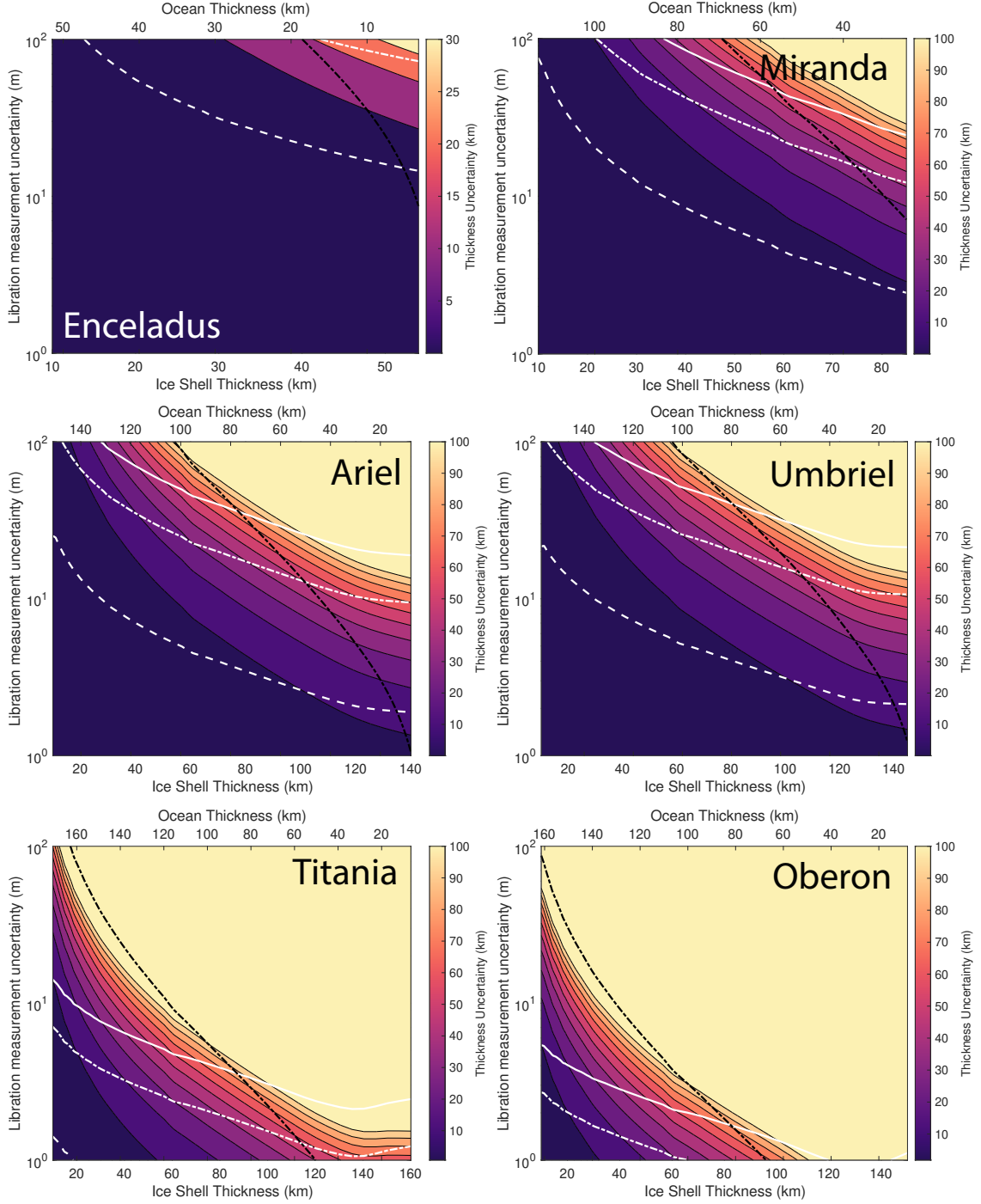
August 21, 2024, 2:39pm

Figure S2. Ice shell/ocean thickness uncertainty as a function of shell/ocean thickness and libration amplitude uncertainty and assuming $\rho_{core} = 2400\,\mathrm{kg\,m^{-3}}$. To the right of the dash-dotted black line, uncertainties are larger than the ocean thickness, meaning the presence of an ocean cannot be confirmed. Below the white lines, the ice shell thickness can be constrained to within 10% (dashed white line), 50% (dash-dotted white line), or 100% (solid white line).
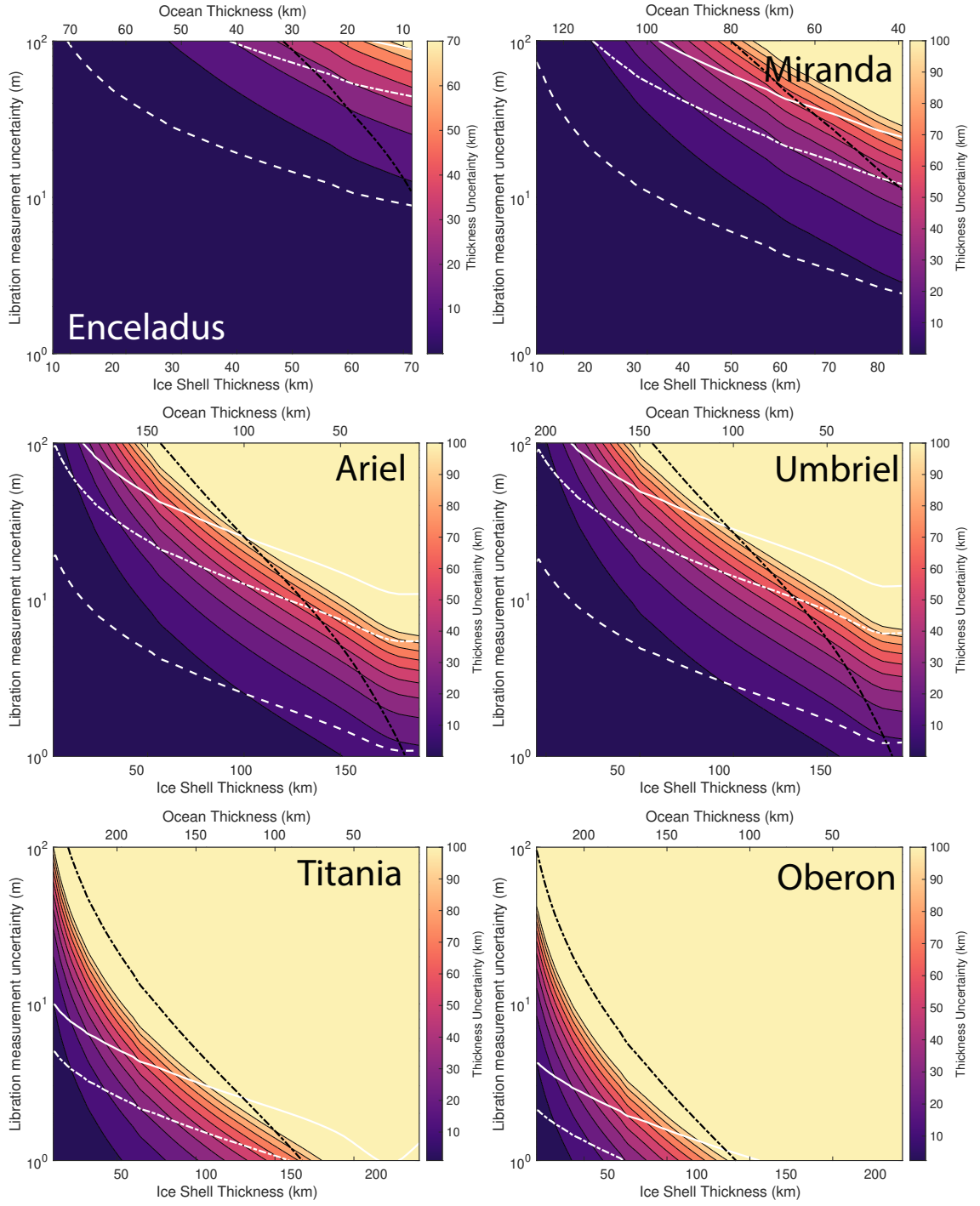
Figure S3. Same as Figure S2 but assuming $\rho_{\text{core}} = 3000\,\text{kg}\,\text{m}^{-3}$.
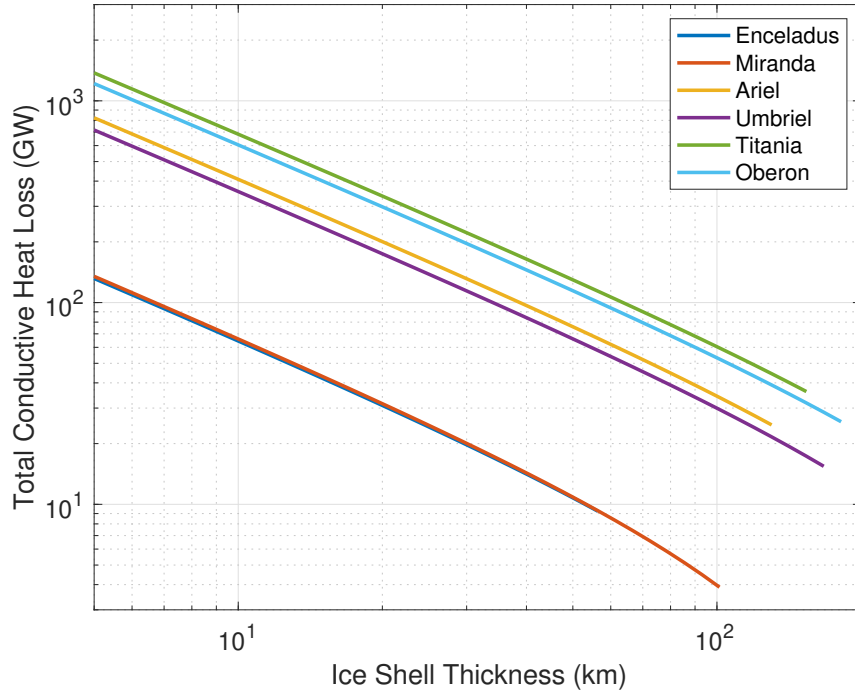
August 21, 2024, 2:39pm

Figure S4. Total heat loss as a function of shell thickness for each body assuming a conductive ice shell with a basal (i.e., melting) temperature of $T = 273\,\mathrm{K}$. See section A.3.
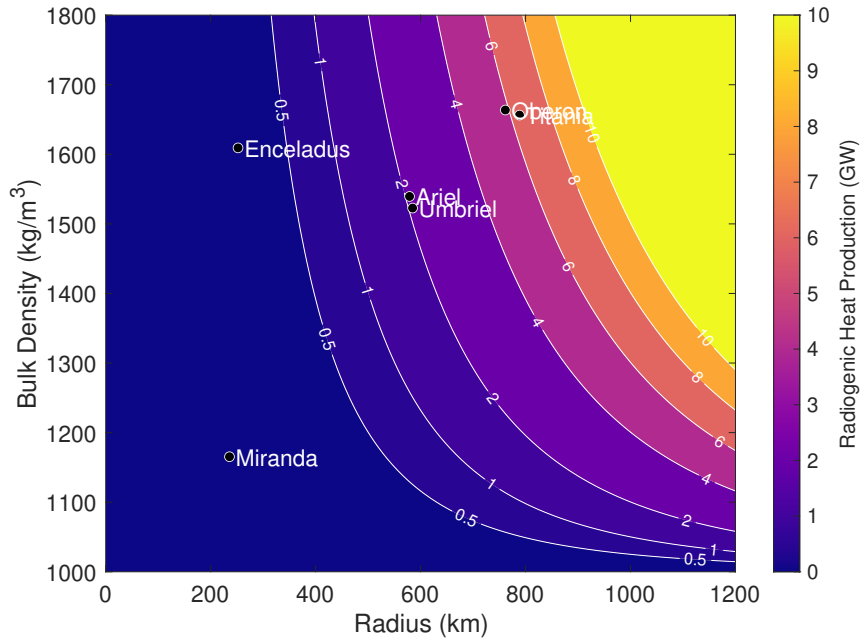

Figure S5. Total radiogenic heat production as a function of radius and bulk density assuming that each body is a mixture of ice and rock (see Text S2 for details).
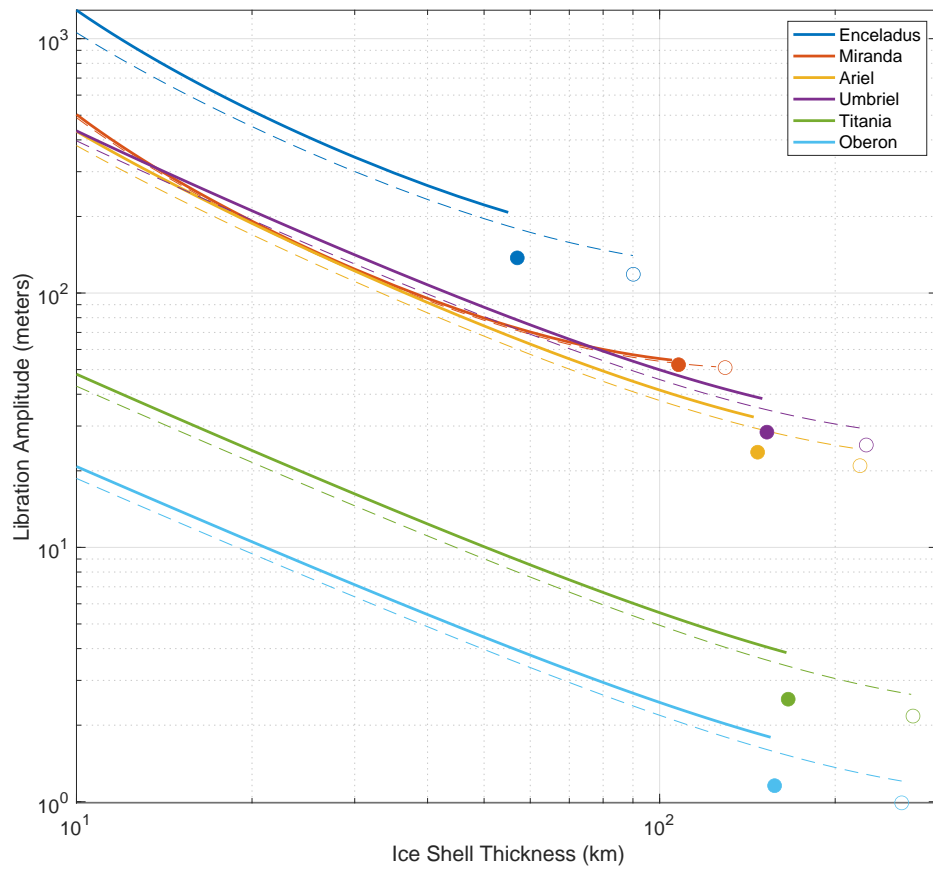
August 21, 2024, 2:39pm

Figure S6.   Same as Figure 1 in the main text but assuming an infinitely rigid ice shell and therefore with libration amplitudes calculated via (A13) rather than (A15).
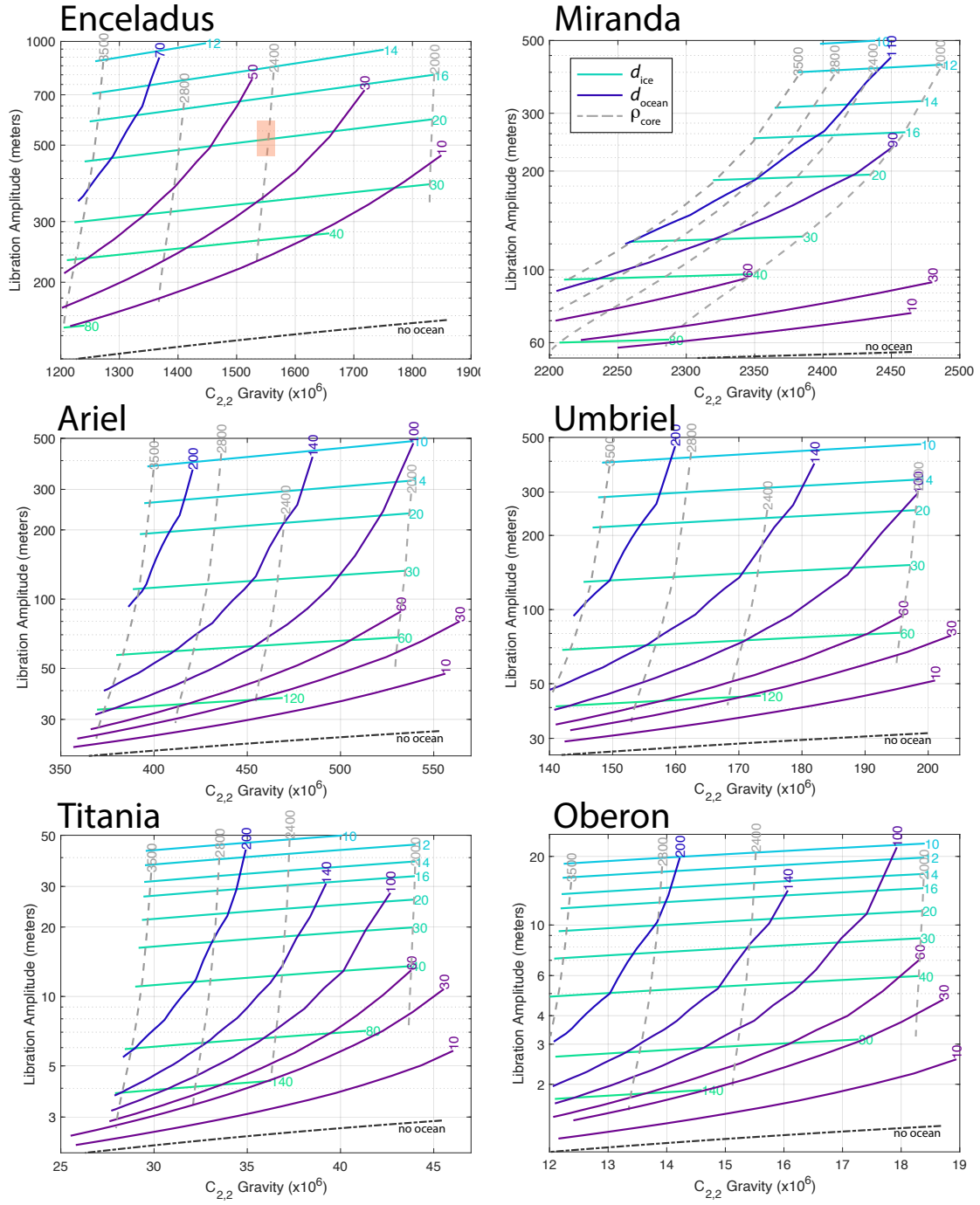
Figure S7.   Same as Figure 2 in the main text but assuming an infinitely rigid ice shell and therefore with libration amplitudes calculated via (A13) rather than (A15).